Evaluating Battery Models in Wireless Sensor Networks

Christian Rohner[1], Laura Marie Feeney[2], and Per Gunningberg[1]

[1] Uppsala University
christian.rohner,perg@it.uu.se
[2] Swedish Institute of Computer Science
lmfeeney@sics.se

Abstract. Recent measurements highlight the importance of battery-aware evaluation of energy efficiency in wireless sensor networks. However, existing battery models been not investigated in the context of the low duty cycle, short duration loads that are typical of sensor networks. We evaluate three battery models with regard to their applicability in the WSN context. Our evaluation focuses on how the models reflect two key battery discharge behaviors, the rate capacity effect and charge recovery. We find that the models handle the former better than the latter and are more sensitive to a load's peak current than to its timing.

1 Introduction

Many energy efficient wireless sensor network (WSN) protocols emphasize minimizing and coordinating the duty cycles of various hardware components. Other WSN applications do load balancing to maintain sensor coverage with a minimum number of active devices. The energy efficiency of these systems is typically evaluated based on measurements or estimates of the total charge (*current* $\times$ *time*) consumed by a device.

However, it is well-known that the available battery capacity is affected by the timing and intensity of the load being applied. Recent measurement results [1] highlight the need for battery-aware methods in evaluating energy efficiency and device lifetime in WSN's. For example, such methods are important for studying load scheduling for battery efficient WSN applications and protocols. If a device has to perform several operations, should it do them consecutively (maximizing the rest time) or separate them (minimizing the load duration)? Similarly, if several devices are sharing responsibility for sensor coverage of an area, what is the optimal length for each device's coverage period?

The practical challenges inherent in directly measuring a battery over its full lifetime suggest that battery modeling will be an essential complement to measurement experiments for battery-aware evaluation in WSN. Moreover, because of complex cross layer interactions, it will be important to incorporate battery models into system and protocol-level simulators operating at network scale.

Battery modeling, especially for Li-ion batteries, is an active research topic. However, there has been very little work studying the effectiveness of existing

battery models for WSN applications, with small, non-rechargeable batteries, low duty cycles and short load durations. In this paper, we investigate three existing battery modeling techniques with regard to their applicability to evaluating WSN protocols and systems: BatteryDesignStudio [2], a commercial electrochemical simulator; KiBaM [3], an analytic model based on a kinetic abstraction; and a hybrid battery model [4] which combines KiBaM with an electrical circuit abstraction.

We focus on how various models reflect two battery discharge behaviors that are particularly important for load scheduling: the rate capacity effect and charge recovery. Our contribution is primarily in the qualitative evaluation of the ability of these models to capture these effects. Our work is unique with regard to evaluating these models in the context of WSN typical loads and in highlighting the potential value of battery-aware energy evaluation to the WSN community.

The outline of this paper is as follows. We first provide some background on battery essentials, illustrated with some of our experimental measurement results on the CR2032 Li-coin cell ($LiMnO_2$) that we use as reference battery for our work. We then describe some background and related work in battery modeling. The core sections of the paper present the three battery modeling tools and evaluate the results we obtained using each. Finally, we conclude that the models are more sensitive to peak current than timing, and that they lack an effective mechanism to track energy efficiency.

2 Background and Experimental Data

This section provides background about batteries and presents measurement data that demonstrate some of the complex behaviors that motivate our work. We also introduce the load patterns used in both the measurements and battery modeling to study the rate capacity effect and charge recovery effects.

2.1 Electrochemical Preliminaries

A battery is a complex electrochemical system: The intensity and timing characteristics of the load affect the amount of charge that can be extracted before the cut-off voltage is reached. Two key battery discharge behaviors are the rate capacity effect and charge recovery: The former refers to the fact that a lower discharge rate (i.e. current) is more efficient than a higher one; more charge can be extracted from the battery before reaching a given cut-off voltage. The latter refers to the fact that an intermittent discharge is more efficient than a continuous one. Because of these effects, different battery loads that use the same total charge do not result in the same device lifetime.

Figure 1 is an oscilloscope trace of the output voltage of a 3V CR2032 battery under load. When a 300Ω ($\sim$10mA) load is applied, the output voltage initially drops sharply (V_{load}), then continues to drop more slowly (V_{min}). When the load is removed, the reverse happens ($V_{recover}$). The voltage $V_{recover}$ approximates the open circuit voltage V_{oc} after a sufficiently long recovery period (hours). The

details of the battery's voltage response depend on the size and duration of the load and the length of the recovery period (i.e. on the rate capacity and charge recovery effects).

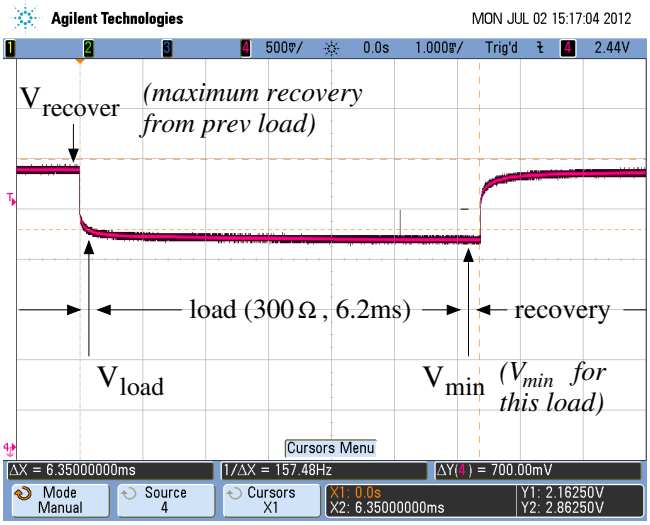

Fig. 1. Battery dynamics during a load

The voltage response also depends on the battery state of charge (SOC). Figure 2 shows how the voltage response to a combination of periodic loads changes over the life of the battery. In this trace, the battery is repeatedly discharged with 1mA continuous load for 11h and allowed to rest for 8.5h. A 22mA pulse load is applied for 10 seconds followed by a rest interval of 30 minutes at the beginning of each load interval. The shape of the voltage response is similar to that in Figure 1. The rate capacity effect is seen in the difference between the battery response to the 1mA and 22mA loads. The voltage response also changes over the lifetime of the battery; the voltage drop becomes both larger and steeper and the recovery slower. Eventually, the battery's output voltage in response to load becomes too low to operate the device correctly; this cut-off value is device dependent. The battery efficiency therefore corresponds to the amount of charge (i.e. useful work) that can be extracted before the cut-off voltage is reached.

2.2 Experimental results

Although these and other battery effects have been extensively studied for many kinds of high-end batteries, the results are very specific to a particular battery chemistry and structure. There is very little data about the discharge behavior of the cheap, non-rechargeable batteries, low duty cycles, short load durations, and relatively high loads typical of WSN's.

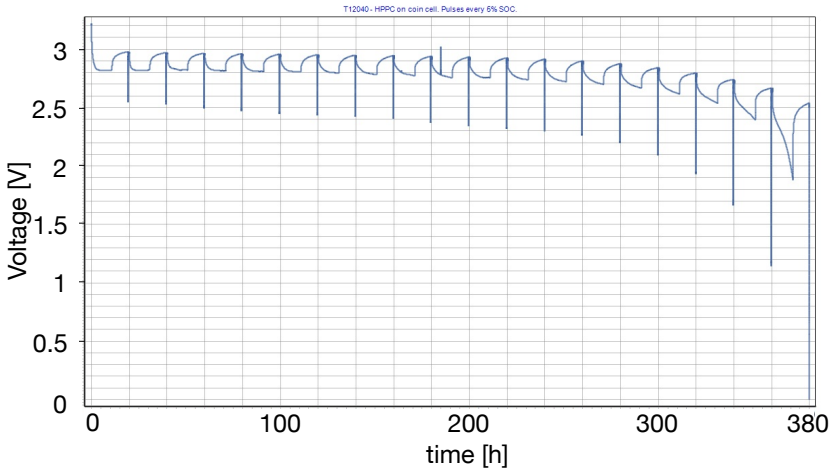

Fig. 2. Battery dynamics over a sequence of loads.

In reality, WSN's exhibit activity patterns that are a combination of periodic and non-periodic events, each with a distinct signature. For example, transmitting a frame involves a sequence of transitions between backoff, listening, and transmitting states. However, it is impractical to control wireless contention and collisions well enough to ensure identical behavior for all frames over a long-term experiment. We therefore work with simple periodic loads, which allow us to isolate key effects and can also act as building blocks for modeling more complex loads.

The load parameters that we use in this paper are shown in Table 1 and are intended to reflect a range of plausible values, without being tied to any specific hardware or protocol. The load values are typical of low bit-rate transceivers such as the RFM TR1001[5]. The load durations are also consistent with low bit-rate frame reception and shorter wakeup/listen durations, while the periods are typical of MAC wakeup schedules. We also include a higher 25mA load, which is typical of sensor operation.

These loads allow us to make comparisons along several axes. For example, CI.3 and I.6 have the same duty cycle and load (i.e. the same time-average current), but I.6 has a longer period. Comparing these allows us to see how absolute load and rest times impact the recovery effect. Similarly, we can compare CI.3 and CI.9, which have the same period and time-average current, but CI.9 has a higher load and smaller duty-cycle. Comparing these allows us to observe the rate-capacity effect, where there is some tradeoff between brief, intense loads and longer duration loads with lower intensity.

We recently built a battery testbed [6] and used it to measure Panasonic CR2023 Li-coin cell batteries. Our automated testbed allows us to apply periodic resistive loads to sets of batteries in a controlled fashion and see how the

name	note	load	duration	period	duty cycle	avg. current
CI.3	low current short period	750Ω ($\sim$4mA)	15 ms	200 ms	7.5%	300 μA
I.6	low current long period	750Ω ($\sim$4mA)	**150 ms**	**2.0 s**	7.5%	300 μA
CI.9	high current short period	120Ω (**$\sim$25mA**)	2.4 ms	200 ms	1.2%	300 μA

Table 1. Battery loads used in this paper.

voltage response evolves over time. Our results [1] are one of the first battery measurement studies that focuses on WSN scenarios.

Figure 3 shows results of discharging batteries according to the three load patterns listed in Table 1. The voltage under load (V_{min}) is shown for each load pattern, the open circuit voltage (V_{oc}, approximated by $V_{recover}$) is shown for CI.3. For load patterns with similar time-averaged energy consumption, the variation in available capacity is around 10-15%, depending on cut-off voltage. The results confirm the importance of battery-aware evaluation and suggest that a shorter load duration is more battery efficient.

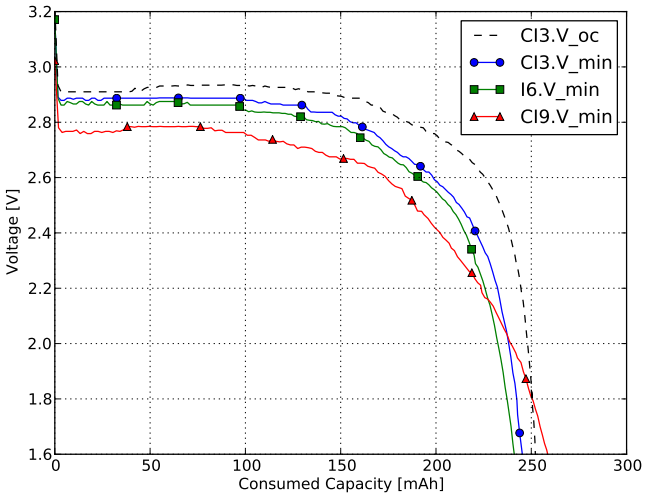

Fig. 3. Experimental data from our battery testbed. The mA-h that can be taken from the battery (at a given voltage) depends on the load pattern. CI9 has a slightly shorter load duration (mean current 262μA) due to a limitation in the testbed.

3 Battery Modeling and Related Work

Battery modeling and simulation is a very active topic [7]. As we have noted earlier, this work is mostly in the context of high-end Li-ion batteries, such as those used in electric vehicles. We roughly divide battery simulation into two categories: Electrochemical simulations model the physical processes in the battery, while analytic simulations use simpler abstractions to represent the battery's response to load.

Electrochemical simulation directly models the physical processes in the battery, based on its detailed chemical and structural properties. Although such models are considered "gold-standard", they have some disadvantages: They have a large number of highly detailed parameters describing the battery chemistry and physical structure. A simulation model is defined not just for a given battery chemistry or type of battery; its parameters are manufacturer-specific. These simulators are also very computationally intensive and their mathematical structure can be difficult to integrate with common discrete-event WSN simulators.

Analytic models replace complex physical models with much simpler representations of battery response to load. These are based on non-electrochemical abstractions, such as electrical circuits, kinetics, diffusion and stochastic processes. These abstractions are therefore more generic and more tractable than models of physical processes, but they present some non-trivial challenges in parameterization. Unlike physical parameters such as electrolyte concentration or surface area that are well-defined properties of a particular battery, abstract parameters such as diffusion constants have no physical reality. These parameters therefore need to be constructed from experimental data.

Perhaps the best known analytic model is the Rakhamatov model [8], which models the battery response as a diffusion process. This work was directed toward the rechargeable Li-ion battery found in early Wi-fi equipped mobile devices. Its short battery lifetime made it possible to define a practical parameterization process and perform some limited validation experiments, as well as simulation using Dualfoil[9] electrochemical simulator.

The Kinetic Battery Model (KiBaM) [3] is an analytic model that uses kinetics to model the battery state in terms of flow between two charge wells, representing bound and available charge. It has been shown that KiBaM is an approximation of the Rakhmatov model [10]. Section 5 describes KiBaM and our experience using KiBaM in detail.

Another class of analytic models uses as an electrical circuit abstraction. Electrical circuit models [11] represent the battery's voltage response using a combination of RC circuit elements. The model can then be evaluated using conventional circuit simulation tools, making it particularly suitable for combining with hardware simulation of the WSN device itself. Section 6 describes our experience with a hybrid model [4] that combines an electrical circuit model with KiBaM.

More recently, a stochastic battery model was proposed in [12]. Although the work was intended for WSN environments, the batteries studied in this

work were rechargeable NiMH batteries. The measurement studies used for both parameterization and evaluation of the model had high duty cycles of 40-90%. By contrast, our work uses duty cycles that are more realistic for WSNs.

In addition to our work on models, there have been some measurement studies of CR2354 Li-coin cells [13, 14]. Both of these studies used much higher loads than typical WSNs, with duty cycles ranging from 25-100%. Their results showed the impact of rate capacity and charge recovery effects on available capacity. Compared to a straightforward calculation of energy consumption as *current* × *time*, the available capacity was seen to differ by as much as a factor of four.

4 Electrochemical Model

Models for $LiMnO_2$ cells have recently been added to a well-known commercial electrochemical simulator, BatteryDesignStudio [2, 15]. We configured our experiments in BatteryDesignStudio using its builtin model of a CR2032 coin-cell battery manufactured by Varta. This battery is similar to the Panasonic CR2032 batteries used in our experiments, but has a slightly larger nominal capacity (240mA-h vs 225mA-h). The simulator was configured to model the periodic load patterns from the experiments described in Table 1.

Due to the computational complexity of the simulation and large number of load events in our experiments (experiment CI.3 has a 200ms period, or more than 20M loads over 1200 hours), the runtime of the simulation turns out to be close to real-time (i.e., ∼50 days). To speed up the simulation, we configured the simulator to drain 60% of the battery capacity with a small continuous load of 0.2mA during a time period equivalent to 30 days and then apply the periodic load pattern for the remaining time. Our rationale is that our earlier experiments indicate that the battery response is approximately constant during the first 60% of its lifetime.

As shown in Figure 4, the electrochemical model used in BatteryDesignStudio captures the rate capacity effect, with CI9 reaching cutoff voltages much earlier than the other load patterns. On the other hand, the model seems to be insensitive to scaling the time period of a cycle (CI.3 and I.6 have the same results). Interestingly, the voltage levels are in general lower than in our measurements on real batteries shown in Figure 3.

As noted above, electrochemical models are computationally expensive. The computations run between two days and four weeks each, depending on the number of load events to be simulated.

5 Kinetic Battery Model

An established way to model the nonlinear capacity dynamics of batteries is to describe the chemical processes by a kinetic process. The analytical Kinetic Battery Model (KiBaM) [3] models the battery as two charge wells, with the charge distributed between the two wells with a capacity ratio c ($0 < c < 1$), as shown in Figure 5. The *available charge well* supplies charge directly to the load

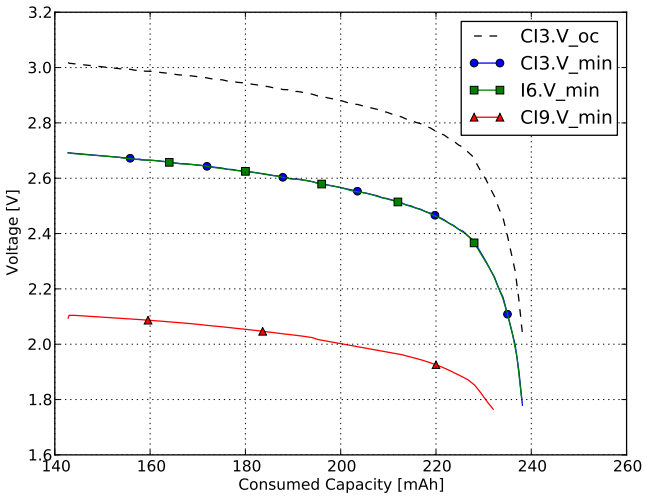

Fig. 4. Battery discharge curve for the electrochemical model in BatteryDesignStudio (note that the x-axis begins with the battery partially drained). Loads CI.3 and I.6 (both 4mA) have the same discharge curve.

and the *bound charge well* supplies charge to the available charge well through a valve. The rate at which charge flows from the bound to the available charge well depends on the valve, characterized by the diffusion parameter k ($(0 < k < 1)$), and the difference between the charge level in each of the two wells, h_1 and h_2. The total charge in the available well and the bound well are $y_1 = ch_1$ and $y_2 = (1 - c)h_2$, respectively. The state of charge of the battery is represented by h_1, and the battery is fully discharged when h_1 becomes zero. That is, the battery can be fully discharged, even if there is (bound) charge remaining.

Intuitively, we see that if the battery is discharged at a higher current, the available charge well is emptied more quickly than it would be if the battery were discharged at a lower current. This reflects the rate capacity effect. At rest, charge flows from the bound charge well to the available charge well until equilibrium $h_1 = h_2$ is reached. Replenishing the available charge well in this way reflects the charge recovery effect.

Following notation in [3], the kinetic process is expressed as:

$$\begin{cases} \frac{y_1(t)}{dt} = -i(t) + k[h_2(t) - h_1(t)] \\ \frac{dy_2(t)}{dt} = -k[h_2(t) - h_1(t)] \end{cases} \tag{1}$$

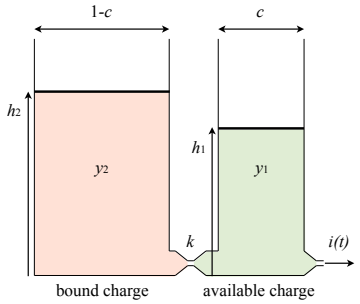

Fig. 5. Kinetic Battery Model

For a constant discharge current of $i(t) = I$, the differential equations (1) can be solved as:

$$\begin{cases} y_1(t) = y_{1,0}e^{-k'(t-t_0)} + \frac{(y_0k'c-I)(1-e^{-k'(t-t_0)})}{k'} - \frac{Ic(k'(t-t_0)-1+e^{-k'(t-t_0)})}{k'} \\ y_2(t) = y_{2,0}e^{-k'(t-t_0)} + y_0(1-c)(1-e^{-k'(t-t_0)}) \\ \qquad\qquad - \frac{I(1-c)(k'(t-t_0)-1+e^{-k'(t-t_0)})}{k'} \end{cases} \tag{2}$$

where $k' = \frac{k}{c(1-c)}$, and $y_0 = y_{1,0} + y_{2,0}$ the charge of the battery at time t_0. The unavailable charge $u(t)$ of the battery can thus be expressed as:

$$u(t) = (1-c)[h_1(t) - h_2(t)]. \tag{3}$$

The available charge can be described as $y_0 - \int i(t)dt - u(t)$.

The paramterization of the KiBaM model is based on the assumption that the delivered capacity under very small current loads corresponds to the initial charge y_0. Conversely, a large constant discharge drains the available charge well with only little charge replenished from the bound charge well ($y_{1,0}$), letting us compute the ratio $c = y_{1,0}/y_0$. The value of k' is determined such that the unavailable charge agrees with experimental results from constant discharge when the cutoff voltage of 2.0V is reached. Since $u(0)$ is zero at the beginning of the experiment and t_{co} is known, k' can be extracted. From our experimental measurements with small (1mA) and large (25mA) constant discharge we concluded $y_0 = 0.243Ah$ and $y_{1,0} = 0.028Ah$, respectively, resulting in to the parameters $c = 0.115$ and $k' = 0.266 \cdot 10^{-3}$.

We modeled our periodic load patterns assuming piecewise constant loads of $I > 0$ followed by rest intervals with $I = 0$, and iterated them over Equation (2) to compute the available charge after every cycle. Because KiBaM models available charge rather than output voltage, we use it to compute the lifetime t^* of the battery, at which the simulation reaches $h_1(t^*) = y_1(t^*)/c = 0$. This computation takes only minutes on an ordinary PC.

In practice, KiBaM captures the rate capacity and charge recovery effects to some extent, with higher sensitivity to charge recovery than rate capacity.

However, the differences hardly have an impact on the expected lifetime of a battery in the chosen parameter space. The battery lifetimes for our load patterns were all in the range $2887069s \pm 9s$ ($\approx 800h$). This lifetime is shorter than that seen in the experiments (835-1083h for 2.0V cut-of voltage) and in the electrochemical model and furthermore shows no significant difference between load patterns.

The reason why the small differences per load do not sum up to a more significant difference over the large number of load cycles is because the amount of unavailable charge converges to the same value for all load patterns already after a few hours of operation. Loads applied after this convergence do not add to a difference between the patterns.

Moreover, the assumption of piecewise constant discharge is not fully accurate. As seen in Figure 1, the voltage level, and thus the charge drawn is not constant over the duration of a load. The higher the load, and the lower the state of charge, the larger the difference between V_{load} and V_{min}. Such behavior will make a difference for the rate capacity effect and can, for example, be captured with equivalent circuit models as shown in the next section.

6 Hybrid Battery Model

An electrical circuit model has two components: The Thevenin component is a sequence of RC circuits that models the transient response to load. The SoC component models the non-linear variation in battery's open circuit voltage as a function of the state of charge. This can be done within the circuit model by including an active element such as a current-controlled voltage source or it can be computed using some other method. The hybrid electrical circuit model described in [4] uses KiBaM to track the state of charge, as shown in Figure 6.

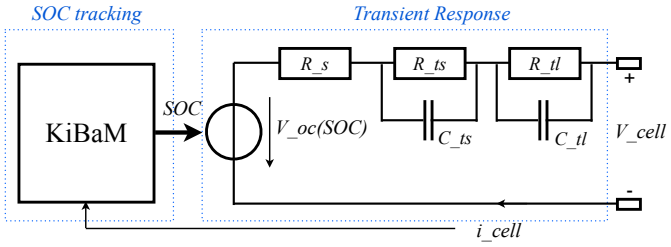

Fig. 6. Hybrid Battery Model

The RC circuits define the transient response to load changes. The circuit parameters define both the cell voltage V_{cell}, and the transient response given by the time constants $\tau_s = R_{ts}C_{ts}$ and $\tau_l = R_{tl}C_{tl}$, which represent the short- and long-term responses, respectively. The larger the time constants, the slower the response.

The cell voltage V_{cell} can be calculated as:

$$V_{cell}(t) = V_{oc}(SOC) - i_{cell}(t) \cdot R_s - V_{transient}(t) \tag{4}$$

For a period in which the battery cell is first discharged with a constant current $i_{cell}(t) = I$ for time t_d, and then rests (i.e., $i_{cell}(t) = 0$), the transient voltage $V_{transient}(t) = V_{ts}(t) + V_{tl}(t)$ is

$$V_{ts}(t) = \begin{cases} R_{ts}I(1 - e^{-t/\tau_s}) & t < t_d \\ V_{ts}(t_d)e^{-(t-t_d)/\tau_s} & t > t_d \end{cases} \qquad V_{tl}(t) = \begin{cases} R_{tl}I(1 - e^{-t/\tau_l}) & t < t_d \\ V_{tl}(t_d)e^{-(t-t_d)/\tau_l} & t > t_d \end{cases} \tag{5}$$

Both the circuit parameters and the open circuit voltage V_{oc} depend on the state of charge. Empirical measurements suggest the behavior described in equations 6 and 7, following the notation in [4]:

$$V_{oc}(SOC) = a_0 \cdot e^{-a_1 SOC} + a_2 + a_3 SOC - a_4 SOC^2 + a_5 SOC^3 \tag{6}$$

$$\begin{cases} R_s(SOC) = b_0 \cdot e^{-b_1 SOC} + b_2 + b_3 SOC - b_4 SOC^2 + b_5 SOC^3 \\ R_{ts}(SOC) = c_0 \cdot e^{-c_1 SOC} + c_2 \\ C_{ts}(SOC) = d_0 \cdot e^{-d_1 SOC} + d_2 \\ R_{tl}(SOC) = e_0 \cdot e^{-e_1 SOC} + e_2 \\ C_{tl}(SOC) = f_0 \cdot e^{-f_1 SOC} + f_2 \end{cases} \tag{7}$$

The negative exponential behavior of the circuit parameters reflects the increasing internal resistance (R_s) and slower reactive behavior (RC components) of the battery with decreasing SOC.

The model parameters are battery and temperature dependent and have to be determined experimentally. Our procedure is based on the one used in [4], where the parameterization is derived from the battery's recovery from a pulse load, as measured at various states of charge.

To do these measurements, we use the load pattern described in Figure 2. The battery is discharged with 1mA continuous load for 11h, then allowed to rest for 8.5h. This load slowly discharges 5% of the battery capacity, minimizing the impact of rate capacity effect, and the rest period allows for charge recovery. A 22mA pulse load (close to the maximum rated load for the CR2032 battery) then is applied for 10s and removed. The immediate voltage increase when the load is removed gives the internal resistance, while $V_{oc}(SOC)$ is estimated using exponential curve fitting on the voltage recovery curve. This also allows us to determine the two transient time constants τ_s and τ_l at the specific SOC.

At the end of this procedure, the circuit parameters at the different SOC levels are least square error fitted by Equations 6 and 7 to estimate the model parameters. Table 2 summarizes the model parameters obtained for the Panasonic CR2032 cell at room temperature.

We applied the battery loads defined in Table 1 to the hybrid battery model to evaluate its ability to capture the rate capacity and charge recovery effects.

V_{oc}	$a_0 = 1.31$	$a_1 = 0.050$	$a_2 = 1.20$
	$a_3 = 2.01$	$a_4 = 2.85$	$a_5 = 1.40$
R_s	$b_0 = 76.4$	$b_1 = 11.8$	$b_2 = 22.9$
	$b_3 = -14.0$	$b_4 = -17.4$	$b_5 = -15.3$
R_{ts}	$c_0 = 37.2$	$c_1 = 16.9$	$c_2 = 3.06$
C_{ts}	$d_0 = -0.468$	$d_1 = 5.33$	$d_2 = 0.370$
R_{tl}	$e_0 = 21.2$	$e_1 = 12.2$	$e_2 = 3.06$
C_{tl}	$f_0 = -5.43$	$f_1 = 4.58$	$f_2 = 5.00$

Table 2. Battery model parameters for the Panasonic CR2032 derived from the battery's recovery from 10s pulses load at 22mA (c.f., Figure 2). These values are used in Equations (6) and (7)

The simulation runtime is around one hour on a PC, using high time resolution to capture the load pattern. The results shown in Figure 7 indicate that the hybrid model captures the rate capacity effect (CI3 vs CI9), which is visible in the voltage level and in the shape of the curve at low SOC. The higher peak current load in CI9 causes the voltage to be lower than in CI3 in the beginning of the experiment and CI3 does not drop equally distinctly at the end. However, like the electrochemical model, the hybrid battery model cannot distinguish between two battery loads with the same peak current load and duty cycle (CI3 and I6). The time constants of the transient response are on the order of 1s and 15s, which is significantly longer than the load duration (2-150ms), so they have have little impact.

Further investigation is needed to understand the sensitivity of model parameters on the current and timing. Results from Chen, et al. [11] show that the parameters of NiMH batteries strongly depend on current, while parameters of polymer Li-ion batteries don't. From our measurements on the CR2032, we have indications that the parameters indeed are sensitive to current, with the time constants getting larger (and thus less relevant for WSN) for lower currents.

Looking at the consumed capacity, the hybrid battery model does not favor any of the battery loads. This observation is expected as all the loads have the same time-average current driving the SOC tracking based on KiBaM. However, the result differs from our observations in the experiments and electrochemical model where the rate capacity effect has an impact on the consumed capacity.

7 Conclusions and future work

In this paper, we present measurement data motivating battery-aware evaluation of energy efficiency in WSN protocols and applications. However, this functionality is not currently provided by existing tools for evaluating WSN performance, nor have existing battery models been investigated in the WSN context, which is characterized by low duty cycles and short duration loads.

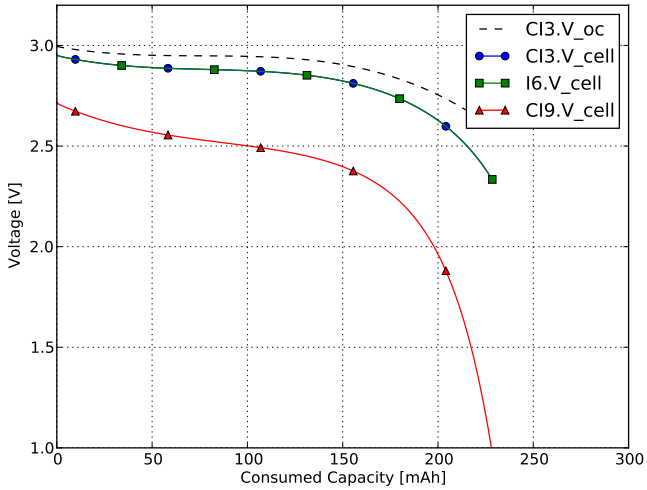

Fig. 7. Results from the Hybrid Battery Model. Loads CI.3 and I.6 (both 4mA) have the same discharge curve.

We have evaluated three well-known battery models using a parameterization based on the CR2032 Li-coin cell battery and three test loads with load values typical of WSN applications. Both BatteryDesignStudio's electrochemical model and the hybrid KiBaM-electrical circuit model capture the rate capacity effect. However, neither of these models seems to capture the effect of load timing, at least for the short load durations and recovery times used in our tests. KiBaM, which is the simplest of the three models, does not show any significant difference in battery lifetime among the three test loads.

The electrochemical model, which is the most complex and computationally expensive of the three models, is sensitive to the rate capacity effect, but not sensitive to timing aspects. The hybrid model behaves similarly, but cannot differentiate energy efficiency (i.e., consumed capacity) of the load patterns.

Because this work opens an area that has not been widely considered in the WSN community, there are many opportunities for future work. Most important is developing better understanding of the models' limitations with respect to modeling timing aspects. Further studies of the parameterization and its sensitivity analysis are also needed.

In the longer term, incorporating battery modeling into existing simulation and modeling tools presents a number of interesting challenges. We expect that the availability of tools for battery aware evaluation of WSN applications and systems will also enable new approaches in both software and hardware design.

Acknowledgements

This work was partly carried out within the Uppsala VINN Excellence Center for Wireless Sensor Networks WISENET, partly supported by VINNOVA, the Swedish Governmental Agency for Innovation Systems.

References

1. Feeney, L.M., Andersson, L., Lindgren, A., Starborg, S., Ahlberg Tidblad, A.: Poster abstract: Using batteries wisely. In: ACM Conf. on Embedded Networked Sensor Systems (Sensys). (2012)
2. Battery Design LLC: Battery design studio http://www.batsdesign.com.
3. Manwell, J., McGowan, J.: Lead acid battery storage model for hybrid energy system. Solar Energy **50**(5) (1993)
4. Kim, T., Qiao, W.: A hybrid battery model capable of capturing dynamic circuit characteristics and nonlinear capacity effects. IEEE Transactions on Energy Conversion **26**(4) (2011)
5. RF Monolithics, Inc.: TR1001 `http://www.rfm.com`.
6. Feeney, L.M., Andersson, L., Lindgren, A., Starborg, S., Ahlberg Tidblad, A.: Poster: A testbed for measuring battery discharge behavior. In: 7th ACM Int'l Workshop on Wireless Network Testbeds, Experimental Evaluation & Characterization (WiNTECH). (2012)
7. Rao, R., Vrudhula, S., Rakhmatov, D.: Battery modeling for energy aware system design. IEEE Computer **36**(12) (2003)
8. Rakhmatov, D.: Battery voltage modeling for portable systems. ACM Trans. on Design Automation of Electronic Systems (TODAES) **14**(2) (2009)
9. Fuller, T.F., Doyle, M., Newman, J.: Simulation and optimization of the dual lithium ion insertion cell. Journal of the Electrochemical Society **141**(1) (1994)
10. Jongerden, M.R., Haverkort, B.R.: Which battery model to use? IET Software **3**(6) (2009)
11. Chen, M., Rinćon-Mora, G.: Accurate electrical battery model capable of predicting runtime and iv performance. IEEE Transactions on Energy Conversion **21**(2) (2006)
12. Chau, C., Qin, F., Sayed, S., Wahab, M., Yang, Y.: Harnessing battery recovery effect in wireless sensor networks: Experiments and analysis. IEEE Journal on Selected Areas in Communications **28**(7) (2010)
13. Park, C., Lahiri, K., Raghunathan, A.: Battery discharge characteristics of wireless sensor nodes: An experimental analysis. In: IEEE Conf. on Sensor and Ad-hoc Communications and Networks (SECON). (2005)
14. Park, S., Savvides, A., Srivastava, M.B.: Battery capacity measurement and analysis using lithium coin cell battery. In: Int'l Symp. on Low Power Electronics & Design (ISLPED). (2001)
15. Yeduvaka, G., Spotnitz, R., Gering, K.: Macro-homogenous modeling of commercial, primary Li/MnO2 coin cells. ECS (Electrochemical Society) Trans. **19**(16) (2009)